Veterinary Microbiology 236 (2019) 108389

Contents lists available at ScienceDirect

Veterinary Microbiology

journal homepage: www.elsevier.com/locate/vetmic

Short communication

Insights into the chicken bursa of fabricius response to Newcastle disease virus at 48 and 72 hours post-infection through RNA-seq

Xiangwei Wang, Yanqing Jia, Juan Ren, Haijin Liu, FathalrhmanEisa Addoma Adam, Xinglong Wang*, Zengqi Yang*

College of Veterinary Medicine, Northwest A&F University, Yangling 712100, People's Republic of China

ARTICLE INFO

Keywords:
Newcastle disease virus
RNA-seq
Avian bursa of fabricius
Innate immune response
Inflammatory response

ABSTRACT

Newcastle disease virus (NDV) causes significant economic losses to the poultry industry worldwide. As a lymphoid organ, the bursa of Fabricius (BF) plays a pivotal role in destroying invading pathogens. Virulent NDV strains can cause rapid atrophy of the BF; however, there is limited knowledge regarding the BF innate immune response to NDV infection. In this study, we used the virulent NDV strain F48E9 to infect four-week-old chickens and found atrophy of the BF, with severe damage and high NDV viral loads after NDV infection in dying chickens. To better understand the interactions between the host and NDV, we compared the transcriptional profiles at 48 and 72 h following infection with the virulent NDV strain F48E9 using RNA-seq. We identified a total of 1498 differentially expressed genes (DEGs), which were enriched in a variety of biological processes and pathways according to Gene Ontology (GO) and Kyoto Encyclopedia of Genes and Genomes (KEGG) pathway enrichment analyses. The enriched pathways were associated with innate immune and inflammatory responses as well as metabolism-related signalling pathways. Excessive inflammatory and innate immune responses induced by the NDV strain may be related to severe BF damage. The global survey of changes in gene expression performed herein provides new insights into complicated molecular mechanisms underlying the interaction between NDV and chickens and will enable the use of new strategies to protect chickens against NDV.

1. Introduction

Newcastle disease (ND) is one of the most contagious infectious diseases in the poultry industry (Spradbrow, 1988). After the first report in 1926, ND was rapidly spread around the world. The disease is caused by Newcastle disease virus (NDV), which belongs to the genus Avulavirus of the Paramyxoviridae family and has a non-segmented, negative-sense, single-stranded RNA genome that contains six genes in the order of 3′-NP-P-M-F-HN-L-5′ and produces two non-structural proteins, V and W, by RNA editing (Steward et al., 1993). Although the use of vaccines controls the outbreak of ND in large areas, wild NDV is frequently discovered in commercial chickens that were previously immunized with NDV vaccines (Dimitrov et al., 2017).

Understanding the host response to NDV infection is necessary to generate improved solutions to combat this devastating disease. Examination of host mRNA expression after challenge provides insight into host-pathogen interactions. Previous studies that used quantitative PCR (qPCR) to investigate gene expression levels in host tissues in response to infection with various NDV strains have reported different cytokine expression levels depending on the strain (Rue et al., 2011; Hu et al., 2015). The bursa of Fabricius (BF) is the central lymphatic organ of humoral immunity, and the micro-environment it provides is the main site for the development and differentiation of B lymphocytes (Glick, 1991). Mature B lymphocytes migrate out through the peripheral blood and enter the spleen and other lymphatic organs. When stimulated by external antigens, the mature B lymphocytes will differentiate and proliferate into plasma cells, synthesize antibodies, and play a role in humoral immunity (Glick, 1991). If this organ is removed during the embryonic stage, antibody production is compromised, leading to immunosuppression (Glick, 1991; Alitheen et al., 2012). Several reports have shown that virulent NDV strains can cause rapid atrophy of the BF (Wakamatsu et al., 2006; Kristeen-Teo et al., 2017). However, to our knowledge, no transcriptome profile of the BF following NDV infection has yet been established.

To better understand the interactions between the host and NDV, we analysed transcriptional profiles at 48 and 72 h following infection with the virulent NDV strain F48E9 infection using RNA-seq. The sequenced segments were compared and screened for differentially expressed

* Corresponding authors.
E-mail addresses: wxlong@nwsuaf.edu.cn (X. Wang), yzq8162@163.com (Z. Yang).

https://doi.org/10.1016/j.vetmic.2019.108389
Received 8 April 2019; Received in revised form 12 August 2019; Accepted 12 August 2019

immune-related genes using the GO and KEGG databases in the National Center for Biotechnology Information (NCBI). Some of the differentially expressed genes (DEGs) were verified by quantitative real-time PCR (qRT-PCR). This study may provide a foundation for further research on understanding of the pathogenesis of NDV infection and extending the knowledge of the interaction between the host and NDV infection.

2. Materials and methods

2.1. Ethics statement

This study was reviewed and approved by the Ethics Committee at Northwest A&F University. Experiments were carried out in accordance with the approved guidelines.

2.2. Virus and animals

Virulent NDV F48E9 used in this study was conserved in our laboratory and propagated in the allantoic cavities of 10-day-old specific pathogen-free (SPF) embryonated chicken eggs. The viruses were stored at -80℃ until further use.

Three-week-old SPF white leghorn chickens were purchased from Merial Vital Laboratory Animal Technology in Beijing, China, and housed in isolators until use. All animal experiments were performed according to the Animal Care and Use Committee of Shaanxi Province, China.

2.3. Animal experiments

In this study, a total of 20 healthy 4-week-old chickens were randomly chosen and inoculated with 0.2 ml of 2×10^4 plaque-forming units (PFU) of F48E9 via the intranasal route. Following infection, the chickens were euthanized at 0, 24, 48, 72 and 96 h post-infection (hpi) to detect the virus loads in the BF. The other half of the BF of each of two chickens at 0, 24, 48, 72 and 96 hpi was placed in 4% paraformaldehyde for 48 h and then dehydrated, embedded in paraffin, cut into 4-um-thick sections, and stained with haematoxylin and eosin (HE) as previously described (Wang et al., 2017).

2.4. RNA sequencing

Half of the BF of each of two chickens at 48 and 72 hpi and the uninfected group at 48 h and 72 h was rapidly placed in Sample Protector for RNA/DNA (Takara, Dalian, China) to explore the transcriptome. Total RNA from each sample was extracted using TRIzol Reagent (Invitrogen, CA, USA) following the manufacturer's instructions. The purity and concentration of the extracted RNA of each sample were measured by a NanoDrop 2000 (Thermo Scientific, USA). RNA integrity was assessed on an Agilent 2100 Bioanalyzer (Agilent Technologies, USA). Sequencing libraries were subsequently generated using rRNA-depleted RNA with an NEBNext® UltraTM RNA Library Prep Kit for Illumina® (NEB, Ipswich, MA, USA) according to the manufacturer's protocol and then sequenced using an Illumina HiSeq 2500 sequencer (Illumina, San Diego, CA, USA).

2.5. Analysis of differentially expressed genes (DEGs), cluster analysis, and gene ontology (GO) and KEGG enrichment

Host gene transcription was analysed by mapping the clean reads to the chicken reference genome downloaded from NCBI (https://www.ncbi.nlm.nih.gov/genome/?term=chicken) via software Hisat2 (v2.0.1). To detect DEGs, the number of clean reads assigned to a gene was counted using HTSeq v0.6.1 (Anders et al., 2015) and then normalized to the values of fragments per kilobase of exon per million fragments mapped (FPKM) (Trapnell et al., 2010). The differential expression levels among the groups were analysed using the DEGseq R package (1.20.0) (Wang et al., 2010). Corrected p-values (q-values) < 0.005 and $|\log2(\text{fold change})| > 1$ were set as the threshold parameters for significant DEGs. GO-TermFinder was used to identify Gene Ontology (GO) terms that annotated a list of enriched genes with a significant p-value less than 0.05. We used in-house scripts to analyse enrichment of significantly DEGs in KEGG pathways (Kanehisa et al., 2008).

2.6. Quantitative real-time PCR (qRT-PCR) analysis

Quantitative PCR was carried out with a real-time thermocycler (Four-channel, Tianlong, China) using the RealStar Green Fast Mixture (GenStar, Beijing, China) according to the manufacturer's instructions. All reactions were carried out in triplicate. Relative expression of the target mRNAs was calculated using the $2-^{\Delta\Delta CT}$ method as previously described (Livak and Schmittgen, 2001), and the 28S gene was used to normalize the fold changes in expression. All primers used in this study are listed in Supplementary Table S1.

2.7. Statistical analysis

Student's *t*-test was used when only two groups of data were compared. All data are presented as the means and standard deviations (SDs), while the statistical significance of differences is reported as follows: * $p < 0.05$, ** $p < 0.01$. All data are representative of no less than three different experiments, and the data were analysed using GraphPad Prism 5 software (GraphPad Software, Inc., San Diego, CA, USA).

3. Results

3.1. Changes in the Bursa of Fabricius (BF) after NDV infection

Chickens infected with virulent NDV F48E9 showed significant respiratory symptoms as early as 72 hpi, and all chickens were dead at 96 hpi. Anatomical analysis revealed that in addition to causing intestinal bleeding, NDV infection caused significant atrophy of the BF, as observed at 96 hpi (Fig. 1A). Histological analysis of the BF at 96 hpi revealed severe depletion of lymphoid cells in the follicles, while the interstitial space was obvious, infiltrated with inflammatory cells and well packed with fibrinous connective tissues at 96 hpi (Fig. 1 B). Subsequently, we detected the NDV viral loads in the BF using qRT-PCR at different times. The results showed that NDV viral loads were detected at 48 hpi and increased from 72 to 96 hpi (Fig. 1 C). Since the large degree of cell damage occurring in the BF at 96 hpi would substantially mask the immune response, we chose to study NDV-host interactions to compare the BF transcriptome at 48 h and 72 h after NDV infection.

3.2. Host response to NDV infection

By using the Illumina HiSeq platform to better understand the interactions between the BF of chickens and NDV, a total of 723,629,692 raw data were produced between the control group and infection group. To guarantee ideal results for further analysis, raw reads were filtered to move low-quality data, with a total of 689,675,257 clean reads acquired, a mean of 85.83% of which mapped to the chicken reference genome (Supplementary Tables S1). We analysed DEGs between 48 hpi and 72 hpi groups with DESeq2. The transcripts were filtered by the thresholds of p-value < 0.05 and $|\log2(\text{fold change})| > 1$. Under these criteria, 1498 DEGs were identified in the BF after NDV infection. Compared with the control group, the 48 hpi and 72 hpi groups contained 256 DEGs (216 upregulated DEGs and 40 downregulated DEGs) and 1419 DEGs (1132 upregulated DEGs and 287 downregulated DEGs), respectively. These results were clearly

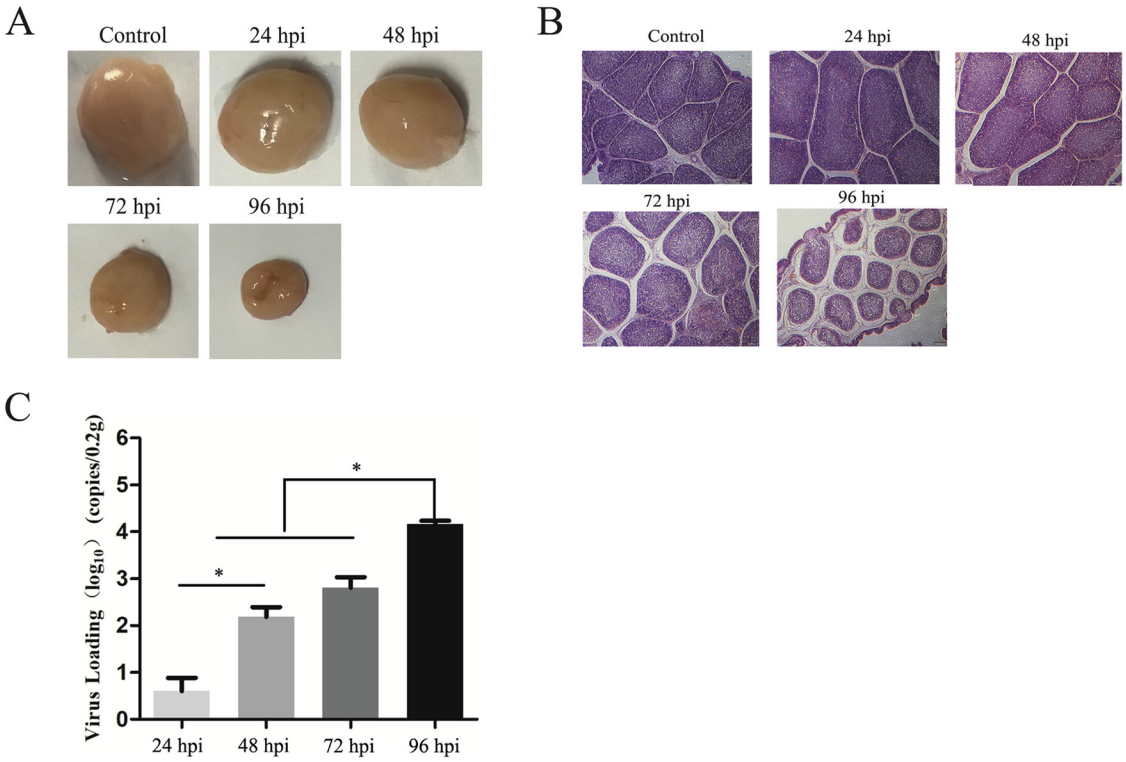

Fig. 1. Changes in the bursa of Fabricius (BF) after NDV infection. (A) Morphological characteristics of the BF of healthy and infected chickens. (B) Histopathological changes of the chicken BF in the control group. (C) The kinetics of NDV viral load in the BF at 24, 48, 72 and 96 hpi were detected using quantitative real-time PCR. The data are expressed as the mean ± standard deviation. The data presented are from three independent experiments, and the result is presented as the mean ± SD. *P < 0.05.

visualized by clustering the samples by differential treatment and by constructing a volcano plot of the DEGs. A list of the DEGs is provided in Supplementary Tables S3 and S4. (Fig. 2)

3.3. GO analysis of DEGs after NDV infection

There was a clear difference in the number of DEGs between the 48 hpi and 72 hpi groups. These DEGs reflected the differential responses of the host to NDV infection at different times. GO analysis of the DEGs was performed to elucidate gene functions. A total of 936 of 1498 (62.48%) gene transcripts were annotated with GO functions. According to the GO functions, these DEGs were classified into the domains biological process, cellular component, and molecular function. The top 20 of GO categories that were significantly enriched in biological process at the two time points are shown in Fig. 3A and B. The three GO terms response to stimulus (GO:0050896), immune system process (GO:0002376) and response to stress (GO:0006950) were significantly enriched at both time points. The DEGs enriched in the significant categories at the two time points are provided in Supplementary Tables S5 and S6.

3.4. Activation of immune and metabolism-related pathways after NDV infection in the BF

KEGG pathway analysis was used as an additional way to explore the function of the DEGs. The significantly enriched KEGG pathways ($p < 0.05$) at 48 hpi and 72 hpi are listed in Supplementary Table S7 and S8. In total, 28 KEGG pathways were identified during the process of NDV infection at these two time points. Among the 28 KEGG pathways, there were nine at 48 hpi and 19 at 48 hpi. Nine of the 28 pathways are associated with metabolism and ten with the immune response. DEGs enriched in immune-related pathways are listed in Table 1 and Table 2. Among these pathways, the RIG-I-like receptor signalling pathway, NOD-like receptor signalling pathway, TLR signalling pathway, and cytokine-cytokine receptor interaction pathway are associated with the innate immune response and the inflammatory response. These results indicate that the BF induces pathways related to immune response, signal transduction, and signal molecules and interaction to resist NDV infection.

3.5. Network analysis of the relationships between DEGs Co-expressed between 48 hpi and 72 hpi

There were 176 DEGs (165 upregulated and 11 downregulated) co-expressed between 48 hpi and 72 hpi (Fig. 4A). Many upregulated genes with known immune functions were involved in the response to NDV, such as the interferon (IFN)-stimulated genes (ISGs) MX1, OASL, RSAD2, and IFITM5; the chemokines CCL4 and CCLI10; and certain interleukin receptors such as IL6ST, IL13RA2 and IL4I1. To predict the interactions of the 176 proteins encoded by the DEGs, we used STRING to generate protein-protein association networks (Fig. 4B). The network was mainly divided into 4 clusters, and the upregulated genes MPEG1, TLR3, IRF7 and EPSTI1 were involved in the most pairs in each cluster, which suggested that they might play an important role in NDV infection. A full list of the genes involved at both 48 hpi and 72 hpi is displayed in Supplementary Table S9.

3.6. Verification of DEGs by qRT-PCR

To further confirm the differential gene expression obtained from the transcriptome sequencing data, a subset of nine unigenes co-expressed during NDV infection at 48 and 72 hpi with annotations from the statistical analysis of the RNA-seq data was selected for qRT-PCR analysis. As shown in Fig. 5, nine genes exhibited concordant regulation in both the RNA-seq and qRT-PCR analyses. These results support that the differential expression identified via RNA-seq is reliable.

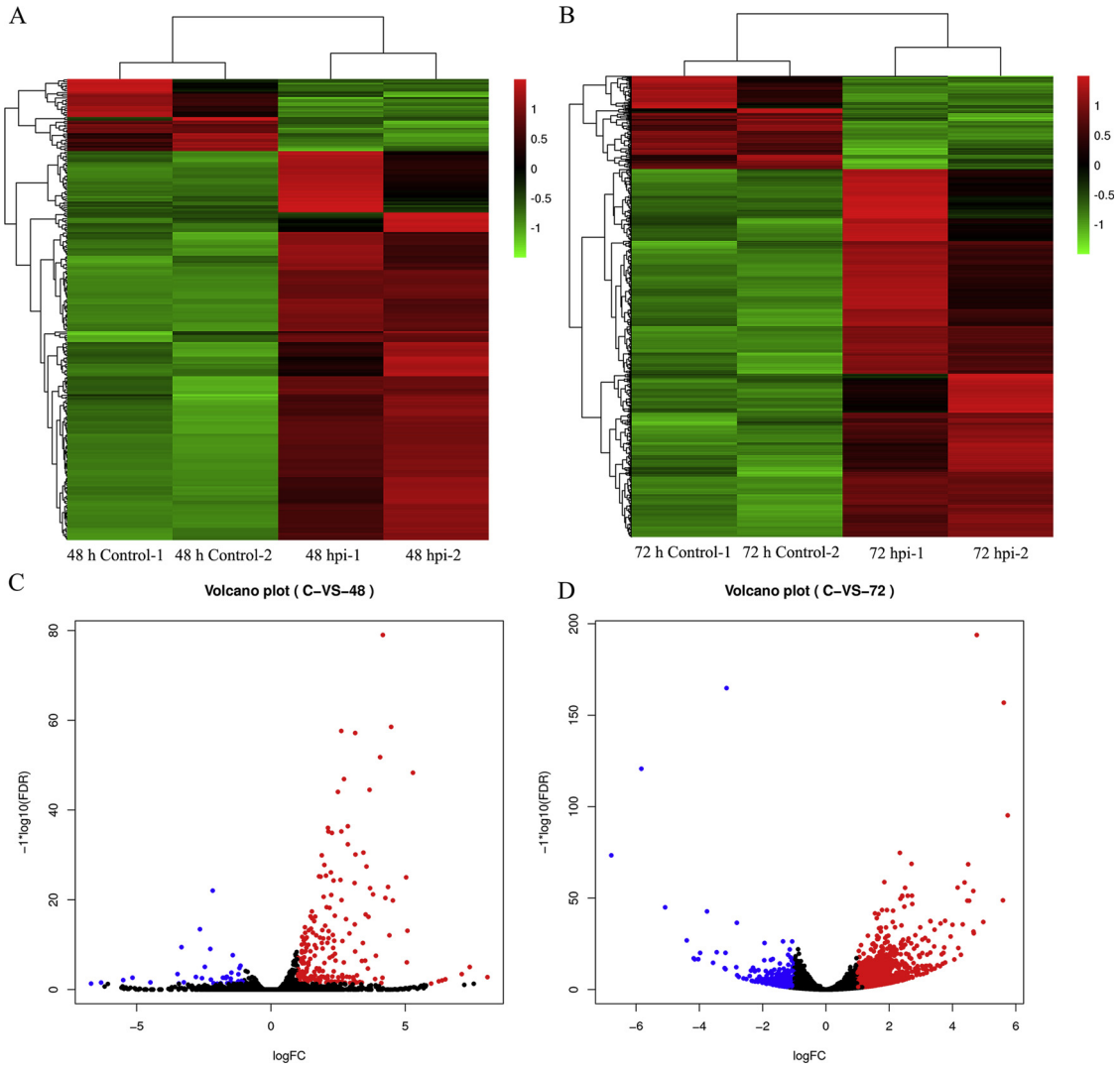

Fig. 2. Analysis of differentially expressed genes (DEGs) of 48 hpi and 72 hpi groups (p-value < 0.01 and fold change > 1). A heat map analysis is used to classify gene expression patterns, and a volcano plot displays the number of DEGs. (A, B) The x-axis represents the experimental conditions. (C) Volcano plot of DEGs between the control and 48 hpi groups. (D) Volcano plot of DEGs between the control and 72 hpi groups. The x-axis indicates the base 2 logarithm of fold change; the y-axis indicates the negative logarithm of the p-value.

4. Discussion

Infection by virulent NDV strains can cause atrophy of the BF in chickens, though the immune response in the BF is rarely reported. Therefore, it is necessary to systemically identify the complex mechanisms of NDV-host interactions in this organ. In this study, we used RNA-seq technology to obtain transcriptome sequencing data from the BF of chickens infected with lethal NDV at 48 and 72 hpi. The global profile of gene expression in the BF provided a good overview of the host response to NDV infection, offering insight into the mechanisms by

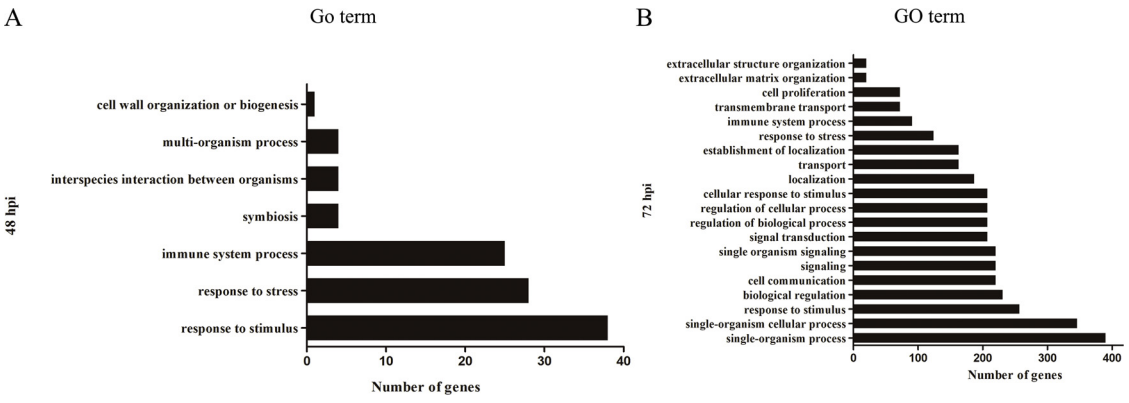

Fig. 3. GO and KEGG enrichment analyses of DEGs. (A, B) Top 20 GO categories in the biological process domain significantly enriched ($p < 0.05$) at 48 and 72 hpi.

Table 1
Immune-related pathways statistically significantly enriched by NDV infection in the BF at 48 hpi.

KEGG pathway	Genes	P value
Influenza A	TRIM25,STAT1,EIF2AK2,TLR3,RSAD2,SOCS3	0.000413818
Herpes simplex infection	STAT1,EIF2AK2,TLR3,SOCS3	0.0219343
Toll-like receptor signaling pathway	STAT1,TLR3,CD86	0.02360195
Intestinal immune network for IgA production	CD86,MADCAM1	0.02612532
RIG-I-like receptor signaling pathway	TRIM25,DHX58	0.04994029

which NDV causes disease and death.

Innate immunity acts as a first line of defence against invading pathogens and is activated when pathogen associated molecular patterns (PAMPs) are recognized by pattern recognition receptors (PRRs) (Yoneyama et al., 2004). KEGG enrichment analysis revealed that DEGs at 48 hpi were mainly enriched in immune-relevant pathways, including the “influenza A pathway”, “Toll-like receptor signalling pathway”, and “RIG-I-like receptor signalling pathway”. In previous studies on chicken lung and chick embryo infected with NDV (Deist et al., 2017; Jia et al., 2018), DEGs were considerably enriched in immune-related pathways. In this study, we found that following NDV invasion of the BF, PRRs, such as MDA5 and TLR3, were significantly upregulated at 48 hpi and activated downstream interferon regulatory factors (IRF3), which translocate into the nucleus upon phosphorylation, activating type I interferons. Interestingly, in our study, type I interferons (IFNα and IFNβ) were not differentially expressed at 48 hpi, although interferon-induced genes (ISGs) were found to be induced. These findings support the observation that NDV non-structural proteins (V proteins) play a role in inhibiting type I IFN production (Motz et al., 2013). Interferons play antiviral roles mainly through the production of ISGs. Consistent with previous reports (Jia et al., 2018; Liu et al., 2018), a large number of ISGs were found at 48 and 72 hpi, of which many have been reported to be involved in antiviral processes, such as OASL, MX1, PML and RSAD2. However, this intense host immune response is unsuccessful in controlling rapidly progressing infection and results in high mortality in chickens. How NDV escapes from the host innate immunity remains to be further studied.

In mammals, cytokine storms, characterized by dysregulated and exaggerated production of inflammatory cytokines, correlates with increased morbidity and mortality during viral infections (Kobasa et al., 2007). Indeed, the inflammatory response is a double-edged sword that plays an important role in tissue metabolism (Brenner et al., 2013). A mild inflammatory response exerts consistent protective effects, whereas excessive inflammation may cause tissue damage. Previous studies have demonstrated that NDV infection can induce a severe inflammatory response (Rue et al., 2011; Hu et al., 2015). In the present study, the KEGG pathway cytokine-cytokine receptor interaction was enriched at 72 hpi, and pro-inflammatory cytokines, including IL1RL1, IL1R2, IL1R1, IL6ST, IL8L2, and IL10, were significantly upregulated at 72 hpi. These results demonstrate that the response of overabundant cytokines to NDV infection is not critical for the efficient elimination of the virus and is insufficient to protect chicken hosts from death. Moreover, it is likely the direct result of an increased viral burden as a consequence of enhanced virulence that in turn results in severe immunopathological damage.

Without the ability of autonomous metabolism, virus replication relies on host cells. With an increasing time of virus invasion, we found that an increasing number of signalling pathways related to metabolism was gradually involved (Tables S7 and S8). Metabolism plays a significant role in interactions between the host and pathogen. Studies indicate that viruses can alter host cellular metabolic networks to promote their own replication (Goodwin et al., 2015; Sanchez and Lagunoff, 2015). Previous studies showed that NDV infection could affect DNA synthesis, thymidine metabolism, and vitamin metabolism (Hand, 1976; Venkata Subbaiah et al., 2015). Interestingly, in our study, we observed that most DEGs enriched in the pathway Amino acid metabolism were upregulated and that most enriched in the pathway Lipid metabolism were downregulated. Previous studies have shown that lipid metabolism plays a vital role in antiviral responses (Reading et al., 2003; Yan et al., 2019). However, the specific molecular mechanism that enables NDV targeting of host cell metabolism to ensure its survival and replication and the interactions between the immune response and metabolic processes in NDV infection need to be further studied.

5. Conclusion

We utilized the RNA-seq platform to screen and identify differentially expressed transcripts in the NDV-infected chicken BF. The DEGs were associated with immune and inflammatory responses as well as metabolism-related signalling pathways. Excessive inflammation and innate immunity induced by NDV caused severe BF damage. This research provides a basis for elucidating the mechanism of virus pathogenesis and virus-host interaction for NDV.

Funding

This work was supported by the National Natural Science Foundation of China (No. 31572538).

Table 2
Immune-related pathways statistically significantly enriched by NDV infection in the BF at 72 hpi.

KEGG pathway	Genes	P value
Cytokine-cytokine receptor interaction	IL10,IL19,PRLR,TNFRSF6B,IL1RAP,IL15,IFNG,MPL,GP130, IL1RL1,IL13RA2,CCR2,RELT,IL1R2,TNFRSF11B,IL1R1, IL2RA,ACVR1C,TNFRSF1A,CCR5,NGFR,TNFRSF1B,CCL4, IFNAR1,BMP2	0.000446703
Influenza A	TRIM25,VDAC1,HSPA8,TLR4,STAT1,IFNG,EIF2AK2,TLR3, IRF3,MX,IFNAR1,STAT2,TNFRSF1A,IFIH1,LOC107049075	0.003605985
Necroptosis	VDAC1,TLR4,STAT1,IFNG,HSP90AB1,EIF2AK2,BCL2,TLR3, ITA,GLUL,PLA2G4F,TNFRSF1A,SQSTM1,STAT4,STAT2,IFNAR1,BIRC3	0.01078567
NOD-like receptor signaling pathway	PSTPIP1,TRPV2,VDAC1,TLR4,STAT1,PLCB4,HSP90AB1, BCL2,IRF3,ITA,GBP,RIPK2,STAT2,IFNAR1,CTST	0.01632843
Intestinal immune network for IgA production	IL10,CD28,IL15,AICDA,CD86,ICOSLG	0.02362932

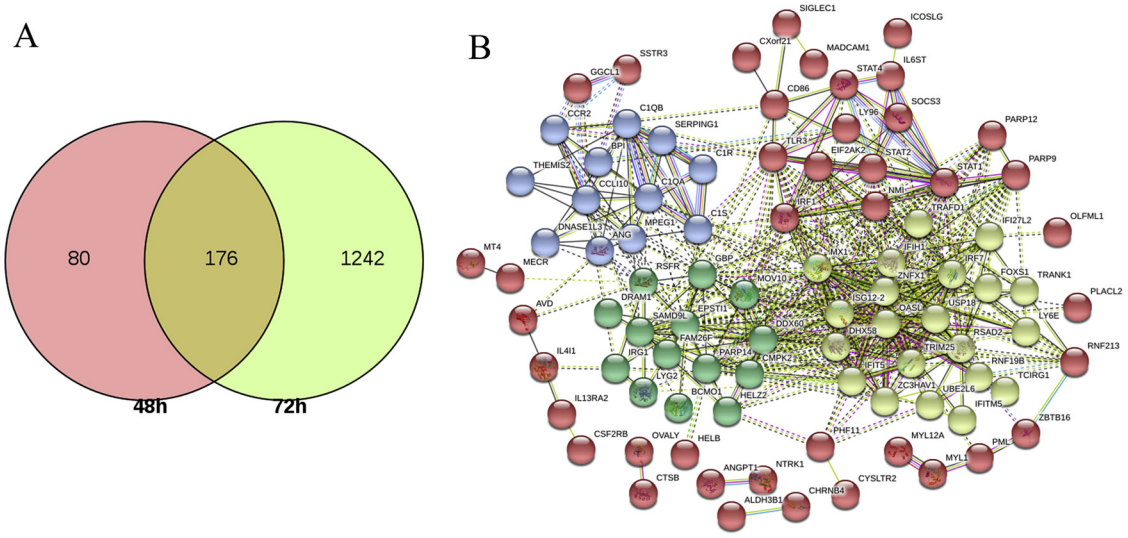

Fig. 4. Co-expressed DEGs between 48 hpi and 72 hpi. (A) A Venn diagram of common DEGs when comparing two groups (control vs 48 hpi and control vs 72 hpi). (B) STRING network analysis of the relationship between proteins co-expressed between 48 hpi and 72 hpi.

Author contributions

Xiangwei Wang and *Zengqi Yang* conceived and designed the experiments, *Xiangwei Wang, Xinglong Wang* and *Haijin Liu* performed the experiments and drafted the manuscript, *Xiangwei Wang* and *Yanqing Jia* analysed the data, *Juan Ren* and *FathalrhmanEisa Addoma Adam* contributed reagents and materials. All authors read and approved the final manuscript.

Declaration of Competing Interest

The authors declare that the research was conducted in the absence of any commercial or financial relationships that could be construed as a potential conflict of interest.

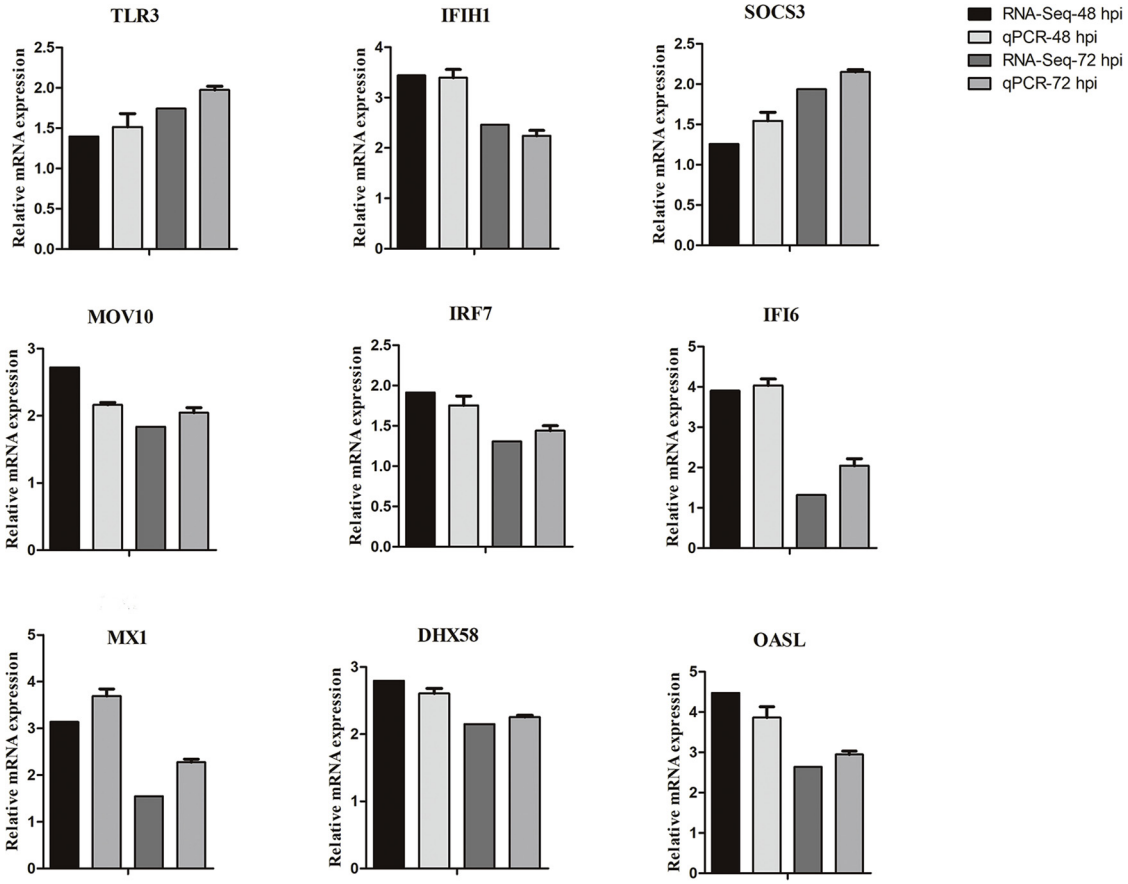

Fig. 5. Verification of the RNA-seq results by quantitative real-time PCR (qRT-PCR). Expression profiles of selected DEGs associated with NDV infection, as determined by qRT-PCR (n = 3). The x-axis shows the annotations of the selected genes. The 28S gene was used for normalization.

Appendix A. Supplementary data

Supplementary material related to this article can be found, in the online version, at doi:https://doi.org/10.1016/j.vetmic.2019.108389.

References

Alitheen, N.B., McClure, S.J., Yeap, S.K., Kristeen-Teo, Y.W., Tan, S.W., McCullagh, P., 2012. Establishment of an in vitro system representing the chicken gut-associated lymphoid tissue. PLoS One 7, e49188.

Anders, S., Pyl, P.T., Huber, W., 2015. HTSeq-a Python framework to work with high-throughput sequencing data. Bioinformatics 31, 166–169.

Brenner, C., Galluzzi, L., Kepp, O., Kroemer, G., 2013. Decoding cell death signals in liver inflammation. J. Hepatol. 59, 583–594.

Deist, M.S., Gallardo, R.A., Bunn, D.A., Dekkers, J.C.M., Zhou, H., Lamont, S.J., 2017. Resistant and susceptible chicken lines show distinctive responses to Newcastle disease virus infection in the lung transcriptome. BMC Genomics. 18, 989.

Dimitrov, K.M., Afonso, C.L., Yu, Q., Miller, P.J., 2017. Newcastle disease vaccines-A solved problem or a continuous challenge? Vet. Microbiol. 206, 126–136.

Glick, B., 1991. Historical perspective: the bursa of Fabricius and its influence On B-cell development, past and present. Vet. Immunol. Immunopathol. 30, 3–12.

Goodwin, C.M., Xu, S., Munger, J., 2015. Stealing the keys to the kitchen: Viral manipulation of the host cell. Trends Microbiol. 23, 789–798.

Hand, R., 1976. Thymidine metabolism and DNA synthesis in Newcastle disease virus-infected cells. J. Virol. 19, 801–809.

Hu, Z.L., Hu, J., Hu, S.L., Song, Q.Q., Ding, P.Y., Zhu, J., Liu, X.W., Wang, X.Q., Liu, X.F., 2015. High levels of virus replication and an intense inflammatory response contribute to the severe pathology in lymphoid tissues caused by Newcastle disease virus genotype VIId. Arch. Virol. 160, 639–648.

Jia, Y.Q., Wang, X.L., Wang, X.W., Yan, C.Q., Lv, C.J., Li, X.Q., Chu, Z.L., Adam, F.E.A., Xiao, S., Zhang, S.X., Yang, Z.Q., 2018. Common microRNA-mRNA interactions in different Newcastle disease virus-infected chicken embryonic visceral tissues. Int. J. Mol. Sci. 19 pii: E1291.

Kanehisa, M., Araki, M., Goto, S., Hattori, M., Hirakawa, M., Itoh, M., Katayama, T., Kawashima, S., Okuda, S., Tokimatsu, T., Yamanishi, Y., 2008. KEGG for linking genomes to life and the environment. Nucleic. Acids. Res. 36, 480–484.

Kobasa, D., Jones, S.M., Shinya, K., Kash, J.C., Copps, J., Ebihara, H., Hatta, Y., Kim, J.H., Halfmann, P., Hatta, M., Feldmann, F., Alimonti, J.B., Fernando, L., Li, Y., Katze, M.G., Feldmann, H., Kawaoka, Y., 2007. Aberrant innate immune response in lethal infection of macaques with the 1918 influenza virus. Nature 445, 319–323.

Kristeen-Teo, Y.W., Yeap, S.K., Tan, S.W., Omar, A.R., Ideris, A., Tan, S.G., Alitheen, N.B., 2017. The effects of different velogenic NDV infections on the chicken bursa of Fabricius. BMC Vet. Res. 13, 151.

Livak, K.J., Schmittgen, T.D., 2001. Analysis of relative gene expression data using real-time quantitative PCR and the 2 (-DeltaDeltaC(T)) method. Methods 25, 402–408.

Motz, C., Schuhmann, K.M., Kirchhofer, A., Moldt, M., Witte, G., Conzelmann, K.K., Hopfner, K.P., 2013. Paramyxovirus V proteins disrupt the fold of the RNA sensor MDA5 to inhibit antiviral signaling. Science 339, 690–693.

Reading, P.C., Moore, J.B., Smith, G.L., 2003. Steroid hormone synthesis by vaccinia virus suppresses the inflammatory response to infection. J. Exp. Med. 19, 1269–1278.

Rue, C.A., Susta, L., Cornax, I., Brown, C.C., Kapczynski, D.R., Suarez, D.L., King, D.J., Miller, P.J., Afonso, C.L., 2011. Virulent Newcastle disease virus elicits a strong Innate immune response in chickens. J. Gen. Virol. 92, 931–939.

Sanchez, E.L., Lagunoff, M., 2015. Viral activation of cellular metabolism. Virology 479-480, 609–618.

Spradbrow, P.B., 1988. Newcastle disease. In: Alexander, D.J. (Ed.), Geographical Distribution. Kluwer Academic Publishers, Boston, pp. 247–255.

Steward, M., Vipond, I.B., Millar, N.S., Emmerson, P.T., 1993. RNA editing in Newcastle disease virus. J. Gen. Virol. 74, 2539–2547.

Trapnell, C., Williams, B.A., Pertea, G., Mortazavi, A., Kwan, G., vanBaren, M.J., Salzberg, S.L., Wold, B.J., Pachter, L., 2010. Transcript assembly and quantification by RNA-Seq reveals unannotated transcripts and isoform switching during cell differentiation. Nat. Biotechnol. 28, 511–515.

Venkata Subbaiah, K.C., Valluru, L., Rajendra, W., Ramamurthy, C., Thirunavukkarusu, C., Subramanyam, R., 2015. Newcastle disease virus (NDV) induces protein oxidation and nitration in brain and liver of chicken: Ameliorative effect of vitamin E. Int. J. Biochem. Cell Biol. 64, 97–106.

Wakamatsu, N., King, D.J., Kapczynski, D.R., Seal, B.S., Brown, C.C., 2006. Experimental pathogenesis for chickens, turkeys, and pigeons of exotic Newcastle disease virus from an outbreak in California during 2002-2003. Vet. Pathol. 43, 925–933.

Wang, L.K., Feng, Z.X., Wang, X., Wang, X.W., Zhang, X.G., 2010. DEGseq:An R package for identifying differentially expressed genes from RNA-seq data. Bioinformatics 26, 136–138.

Wang, X.L., Wang, X.W., Jia, Y.Q., Wang, C.Y., Han, Q.S., Lu, Z.H., Yang, Z.Q., 2017. Adenoviral-expressed recombinant granulocyte monocyte colony-stimulating factor (GM-CSF) enhances protective immunity induced by inactivated Newcastle Disease Virus (NDV) vaccine. Antiviral Res. 144, 322–329.

Yan, B., Chu, H., Yang, D., Sze, K.H., Lai, P.M., Yuan, S., Shuai, H., Wang, Y., Kao, R.Y., Chan, J.F., Yuen, K.Y., 2019. Characterization of the lipidomic profile of human coronavirus-infected cells: Implications for lipid metabolism remodeling upon coronavirus replication. Viruses 11 pii: E73.

Yoneyama, M., Kikuchi, M., Natsukawa, T., Shinobu, N., Imaizumi, T., Miyagishi, M., 2004. The RNA helicase RIG-I has an essential function in double-stranded RNA-induced innate antiviral responses. Nat. Immunol. 5, 730–737.